ARTICLES

Absence of a Signature of Aqueous I($^2P_{1/2}$) after 200-nm Photodetachment of I^-(aq)

Amy C. Moskun‡ and Stephen E. Bradforth*

Department of Chemistry, University of Southern California, Los Angeles, California 90089

Jan Thøgersen* and Søren Keiding

Department of Chemistry, University of Aarhus, Langelandsgade 140, DK 8000 Århus C, Denmark

Received: July 19, 2005; In Final Form: August 3, 2006

Ultrafast pump−broadband probe spectroscopy was used to study the transient photoproducts following 200-nm photodetachment of I^-(aq). Resonant detachment at 200 nm in the second charge-transfer-to-solvent (CTTS) band of I^-(aq) is expected to produce an electron and iodine in its spin−orbit excited state, I*($^2P_{1/2}$). The transients in solution following photodetachment were probed from 200 to 620 nm. Along with strong absorption in the visible region due to solvated electrons and a strong bleach of the I^-(aq) ground-state absorption, a weaker transient absorption near 260 nm was observed that is consistent with a previously assigned ground-state I($^2P_{3/2}$) charge-transfer band. However, no evidence was found for an equivalent I*(aq) charge-transfer absorption, and I($^2P_{3/2}$) was produced within the instrument response. This suggests either that I* is electronically relaxed in less than 300 fs or that excitation in the second CTTS band does not in fact lead to I*. The consequences for previous experimental work where I*(aq) production has been postulated, as well as for halogen electron ejection mechanisms, are discussed. In addition, the broad spectral coverage of this study reveals in the bleach recovery the rapid cooling of the solvent surrounding the re-formed iodide after geminate recombination of the iodine with the solvated electron.

I. Introduction

Photodetachment provides an avenue to generate and study reactive radicals in water from their corresponding stable aqueous anions. Many simple radicals that have been subjected to exhaustive spectroscopic characterization in a vacuum, and whose collisional and reactive properties in the gas phase are also well understood, have not been observed at all in common liquids such as water and the alcohols. For example, the absorption spectra of the ubiquitous CN and HCO radicals that are important in combustion have not been assigned in water.[1−3] The ClO and CS radicals probed in previous femtosecond photolysis studies appear to exhibit very small shifts for their valence-character electronic transitions going from the gas phase into water,[4−6] whereas other species (e.g., NO and O_2) in water develop substantial charge-transfer character in their electronic transitions.[7] The prototypical players in much of small-molecule reaction dynamics, halogen atoms, have not been observed in their spin−orbit excited states in strongly interacting media such as liquid water, and it is unclear how fast electronic relaxation takes place in such simple radicals in solution. In the gas phase, it is known that many halogenated compounds, when photolyzed, lead to spin−orbit-excited halogens,[8−13] so it is of some importance to understand the lifetime of such species in solution and how to detect them.

Our motivation for this study comes from experiments by our two groups on the photodissociation dynamics of ICN. Larsen et al. recently reported a broadband probe study of this system in a single solvent, H_2O.[2] In that study, populations of ground-state I, spin−orbit-excited iodine, I*, and INC were assigned and photochemical yields were evaluated. As part of the study, Larsen et al. attributed a previously unassigned absorption band to I*(aq). In a complementary experiment, Moskun and Bradforth explored the dynamics of the other reaction fragment, the cyano radical, emerging from the reaction and recorded the CN vector correlations with the dissociated ICN. Tracking of the CN population and its vector correlations was carried out, in a number of polar solvents including water, by transient absorption in the 385−400-nm region, near the gas-phase B ← X band.[1,14]

Together, these two experiments shed considerable light on how the dissociation dynamics of this prototypical reaction system are altered by the solvent and reveal many interesting facets of the subsequent behavior of the reaction products. However, spectral assignments made by our two groups are in apparent conflict, particularly for the carrier of the transient absorption in the 320−400-nm band.[15] It is in this spectral region that the single probe wavelength experiments of Moskun and Bradforth are performed. The USC group assigned probe absorption at 387 nm in water to the CN photoproduct.[1] In contrast, the Aarhus group assigned transient absorption in this region to an I*−solvent charge-transfer complex that had not been previously observed and, supported by multiconfigurational

* To whom correspondence should be addressed. E-mail: bradfort@usc.edu (S.E.B.); thogersen@chem.au.dk (J.T.).

‡ Current address: Department of Chemistry, University of California, Irvine, CA 92697.

10.1021/jp053992+ CCC: $33.50
Published on Web 09/02/2006

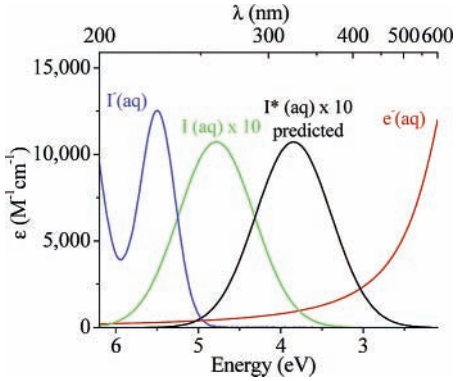

Figure 1. Room-temperature static absorption spectra of I^-(aq) (blue, ref 67) $I(^2P_{3/2})$(aq) (green, ref 26) and e^-(aq) (red, ref 25). The predicted spectrum of the aqueous $I^*(^2P_{1/2})$ (black) absorption from ref 2 is based on Mulliken theory for charge-transfer complexes.

self-consistent field calculations, tentatively assigned an additional shoulder in their dataset to the CN B ← X absorption in water around 450 nm.[2] It is therefore clear that further experiments, where possible, and new calculations[15] are necessary to unambiguously characterize the absorption spectra of the aqueous CN and I* species. Photodetachment of the corresponding anions should allow study of the spectroscopy of both species: in this article, we report results with respect to the I* species.

Figure 1 shows the ground-state absorption spectrum of the aqueous iodide ion. The spectrum is characterized by two absorption features (226 and 194 nm at 30°C) that are assigned to charge-transfer-to-solvent (CTTS) bands. Excitation into each CTTS band is known to produce a solvated electron with high quantum efficiency,[16−18] and it has been assumed, based on the observation that the splitting of the first two aqueous absorption bands almost exactly matches the gas-phase spin−orbit splitting of neutral iodine, that the core fragments produced are $I(^2P_{3/2})$ in the lowest-energy band and $I^*(^2P_{1/2})$ in the second absorption band.[19,20] We present here a comprehensive pump−probe study in which transient absorption probed from the deep-UV through the visible region (a 4.2-eV bandwidth window) were recorded after excitation of I^-(aq) in the second CTTS band at 200 nm. Surprisingly, our results yield no spectroscopic signature of I* after photodetachment in this "I* CTTS" band and provide evidence for substantial and rapid cooling of the surrounding water shells after re-formation of I^- following return of the detached electron to the iodine radical parent.

II. Spectroscopy

Excitation of aqueous iodide at 200 nm is expected to lead to the almost exclusive production of I* and a solvated electron according to the simple argument given in the previous section.[19−22] Figure 1 shows the known and predicted spectra of possible transients (photoproducts and bleaches) relevant to this experiment: I^-(aq), e^-(aq), $I(^2P_{3/2})$(aq), and $I^*(^2P_{1/2})$(aq).[2,23−27] It is to be expected that the pump probe signals arising after excitation of iodide will be dominated by the strong solvated-electron transient absorption and I^-(aq) bleach signals. The absorption spectra of both of these species at equilibrium are well-known.

The thermalized solvated-electron absorption spectrum peaks near 720 nm at 298 K and is very broad. The high-energy side, which lies within the probe window of this study, is well described by a Lorentzian function. Jou and Freeman accurately used this description of the solvated-electron absorption spectrum over a range of temperatures.[25] After the initial electron ejection, the absorption spectrum is known to be red shifted and to then undergo relaxation to an equilibrium spectrum, a process that can be described either as a thermalization involving a time-varying local temperature[28] or alternatively by a non-equilibrium solvation dynamics model.[29] For ejection from aqueous iodide (when excited in the first CTTS band), the initial electron spectrum is shifted by 0.36 eV and undergoes relaxation with a 850-fs characteristic time, as described in detail by Vilchiz et al.[29]

The lowest transition for the ground-state $I(^2P_{3/2})$ atom in a vacuum below 600 nm is at 183.0 nm.[30] This corresponds to the $5p^46s\ (^4P_{5/2}) \leftarrow 5p^5\ (^2P_{3/2})$ transition. The I* atom has a lower-energy transition at 206.2 nm, the $5p^46s\ (^2P_{3/2}) \leftarrow 5p^5\ (^2P_{1/2})$ transition.[30] There are no other I-atom transitions between 200 and 600 nm. In aqueous solution, ground-state $I(^2P_{3/2})$ is known to have a broad absorption at 260 nm due to a charge-transfer interaction with water where the water acts as an electron donor and the I atom is the electron acceptor. The charge-transfer absorption of aqueous $I(^2P_{3/2})$ is shown in Figure 1 and has a maximum extinction coefficient of 1040 M^{-1} cm^{-1}.[26,27]

Larsen et al. used Mulliken's theory of charge-transfer complexes to predict the absorption maximum of I* in aqueous solution.[2,31] Mulliken's theory predicts the charge-transfer absorption maxima as follows

$$h\upsilon = \mathrm{IP} - \mathrm{EA} + \Delta + \frac{2W^2}{\mathrm{IP} - \mathrm{EA} + \Delta} - U \qquad (1)$$

where IP is the vertical ionization potential of the solvent donor, EA is the vertical electron affinity of the solute acceptor, Δ is the stabilization of the excited state relative to the ground state, W is the resonance integral between the ground state and the excited charge-transfer state, and U is the energy difference between the band onset and maximum.[31] Making the assumption that the only change between the two atomic iodine spin−orbit states is the increased electron affinity of $I^*(^2P_{1/2})$ by the spin−orbit splitting, the I* charge-transfer absorption would be expected to be centered near 315 nm. In the absence of other information, the I* band was assumed to have ϵ_{max} and bandwidth values similar to those of the I-atom absorption. Although a good starting point, this treatment might be oversimplistic, as there is a distinct difference in the wave function of the two spin−orbit states: $I(^2P_{3/2})$ has a spherically symmetric wave function, whereas the $I^*(^2P_{1/2})$ wave function has p-like symmetry.[32]

III. Experimental Section

The ultrafast experiments reported here were performed in the laboratories at Aarhus University. The pump−probe transient spectrometer has been described previously.[33] A 1-kHz titanium−sapphire laser system producing 100-fs pulses with an energy of 0.75 mJ was frequency quadrupled to produce the 200-nm pump pulses used to detach the I^-(aq). The 9-μJ 200-nm pump pulse was modulated at 0.5 kHz by a mechanical chopper synchronized to the 1-kHz pulse repetition rate of the laser. The pump pulse was sent through a delay line and focused into the sample by a $f = 50$ cm parabolic mirror. Probe pulses covering the spectral region from 460 to 620 nm were generated using a 400-nm pumped optical parametric amplifier (OPA). Probe pulses from 260 to 460 nm were obtained by frequency doubling the OPA output in a 0.2-mm BBO crystal. The spectral regions from 214 to 300 nm and from 200 to 220 nm were generated

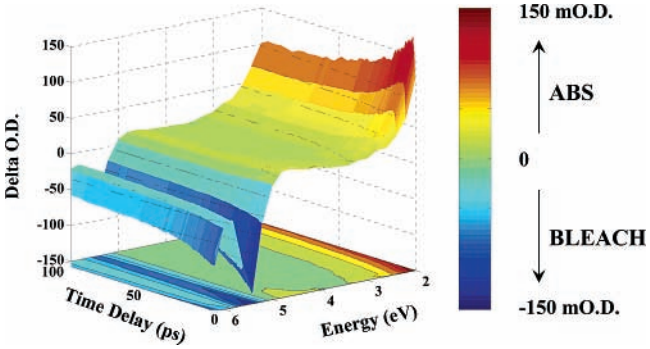

Figure 2. Three-dimensional representation of the induced transient absorption following 200-nm photodetachment of aqueous I^-. The pump−probe transients are scaled to the transient spectrum measured separately at 10-ps delay (see text); the region of pump−probe pulse overlap (the first 400 fs) contributes a large coherent signal and has been excluded from the plot. The false color scale for the magnitude of ΔOD (ranging from bleach to absorption) is shown at the right-hand side. A matching contour map representation is projected below the 3D plot.

by mixing the OPA pulses with residual 400- and 266-nm pulses, respectively. The probe beam was split into two components, the signal and reference pulses. The signal beam was focused into the sample by a $f = 10$ cm CaF_2 lens and probed the sample well within the region defined by the pump beam. The reference beam bypassed the sample. The signal and reference pulses were detected by matched photodiodes and boxcar integrators and then processed by a digital lock-in amplifier referenced to the 0.5-kHz frequency of the mechanical chopper. The resolution of the pump−probe spectrometer was ∼300 fs.

Aqueous 3 mM NaI solution was flowed in a 150-μm-thick jet. The temperature of the sample jet was ∼30 °C as a result of heating of the solution by the mechanical pump. Although no obvious signal from photoproduct surviving between laser shots was detected, the flow of the sample jet was set to ensure that a fresh sample was interrogated at each laser pulse. The further precaution of regular replacement of the sample reservoir was taken to avoid photoproduct buildup, which was further confirmed by UV/visible spectrometry.

Two types of experimental results were obtained: 22 pump probe traces, probing over a wide spectral range from 200 to 620 nm with 0.2-eV probe intervals, and at higher spectral resolution, ∼0.05 eV, transient spectra at 10- and 100-ps time delays. The reproducibility of the latter transient absorption spectra was confirmed by measurements on multiple days. The transient absorption spectrum was measured on a common absorption scale with an uncertainty of less than ±10%. The dominant contribution to this uncertainty comes from variation in the diameter of the probe beam and thus the pump−probe overlap as the probe wavelength was tuned over a 400-nm spectral range. The potential detrimental variation was minimized by keeping the pump beam cross section (∼300-μm-diameter fwhm) much larger than the probe (30-μm-diameter fwhm). The common absorption scale was confirmed by overlapping data points in regions between the different probe generation methods. The error bar on the reported probe wavelength is ±1−2 nm. The two-dimensional data set, shown as a contour plot in Figure 2, was constructed by scaling each transient absorption trace to match the more accurately determined 10-ps-delay transient absorption spectrum in Figure 3a.

The background signal, due to solvated electrons that arise from two-photon ionization of the solvent, was less than 10% of the total signal, i.e., within the error bar of the transient absorption experiment. A power study conducted with a 610-nm probe, near the maximum of the solvated-electron absorption spectrum, verified that one 200-nm pump photon was absorbed by the iodide.

IV. Results

A three-dimensional plot of the pump−probe data from the visible region at 620 nm to the deep-UV region at 200 nm is shown in Figure 2, along with a contour map projection. Three features are obvious in this representation of the data. There is a strong absorption in the visible region of the spectrum where the solvated electron is expected to absorb and a much weaker absorption near 260 nm (band between 4 and 5 eV). A strong transient bleach, resembling the I^-(aq) absorption spectrum, is seen in the UV region of the transient spectrum with a peak at 225 nm (5.5 eV) and another peak below 200 nm (6.2 eV). The time dependence of the iodide-bleach anisotropy was measured at 213 nm (5.8 eV) (data not shown). There was no observable anisotropy[34] probing at this wavelength beyond the time-zero coherent artifact.

The iodide-bleach and solvated-electron absorption signals are an order of magnitude stronger than any other transients. The majority of the transients appear to decay with uniform time scales, over tens of picoseconds with one or two exceptions. The most obvious is a rise component in the visible probe wavelength transients from the thermalization of the solvated electron.[29] Signals from weakly absorbing species (i.e., I or I*) might be obscured by the tails of absorption pertaining to I^-(aq) and e^-(aq). Thus, in our analysis, we remove these contributions to uncover the spectra and dynamics of any weaker transient species.

Let us consider transient spectra at two delays, 10 and 100 ps. The raw transient spectra (open circles) are plotted together with the 30 °C I^-(aq) bleach spectrum (blue), the I($^2P_{3/2}$)(aq) charge-transfer absorption spectrum[26,27] (green), and the fully equilibrated 30°C solvated-electron absorption spectrum[25] (red) scaled by an identical factor (i.e., the same concentration is used for all three) to match the transient signal levels (Figure 3). In addition to the strong e^-(aq) absorption and I^-(aq) bleach, a weaker absorption feature, as noted earlier, is observed around 260 nm. To allow characterization of the spectral signatures of the weaker-absorbing transient species, the solvated-electron and iodide-bleach contributions (the curves indicated on the figure) were subtracted from the transient spectra, and the resulting residuals are shown as solid circles. This subtraction was performed with a strict 1:1 stoichiometric ratio between I^- and e^- After the iodide and electron subtraction, two peaks remain for both 10 and 100 ps, one at 240 nm (5.2 eV) with a broad shoulder around 260 nm (4.7 eV) and the second near 210 nm (5.9 eV). Much of the shoulder at 260 nm is explained by the charge-transfer absorption of the ground-state ($^2P_{3/2}$) iodine atom (green curve) with 1:1:1 stoichiometry. This still leaves residual peaks at 210 and 240 nm to which we will return later. The residual transient absorptions are robust with respect to the probe wavelength errors of 1−2 nm. Importantly, no additional transient absorption is observed at wavelengths longer than 300 nm.[35]

To search for the dynamics of the weaker transients (I and I*) in which we are most interested, we must remove the *time-dependent* contributions from the I^-(aq) bleach and the e^-(aq) absorption signals. This was done in a manner similar to the two time slices discussed above. The I^-(aq) and e^-(aq) contributions to the transient absorption signals were synthesized

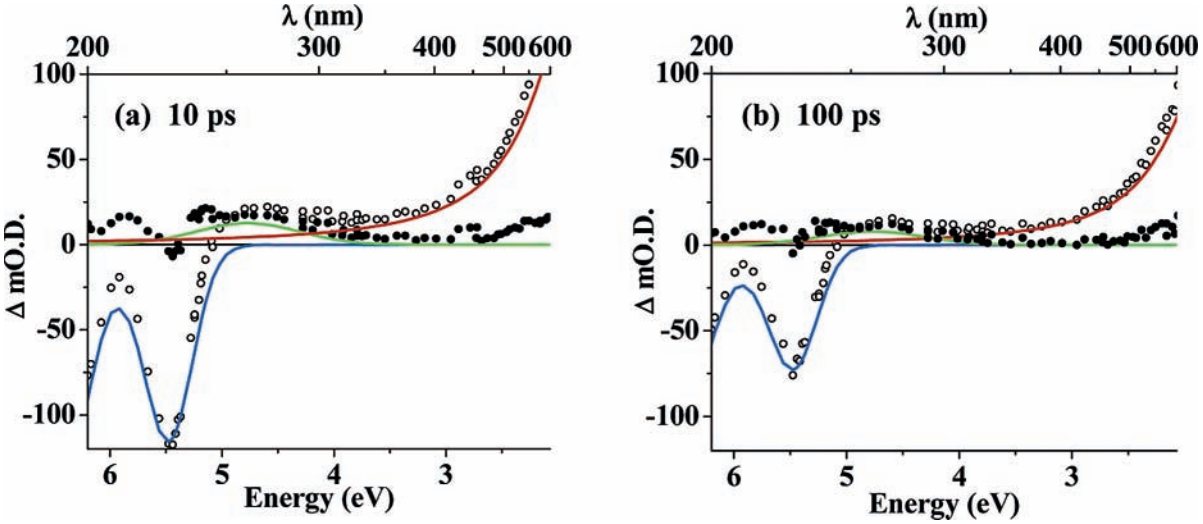

Figure 3. Transient absorption at (a) 10 and (b) 100 ps. The transient spectra (open circles) are dominated by the absorption of the electron (red) in the visible region and the I^-(aq) bleach (blue) in the UV region. The ground-state $I(^2P_{3/2})$ charge-transfer absorption is shown in green. The closed circles represent the transients after the I^-(aq) and e^-(aq) contributions have been subtracted in a 1:1 stoichiometry. The I^-(aq) and e^-(aq) absorption bands shown are for 30 °C (refs 67 and 25) and are those used for the subtraction. The $I(^2P_{3/2})$ charge-transfer absorption (ref. 26) is scaled to 1:1 stoichiometry with the I^-(aq) and e^-(aq) spectra used in the subtraction.

from the known spectra of the two species and subtracted with a 1:1 stoichiometry. In the case of the electron, we used a time-shifting spectrum,[29] and for I^-(aq), we used the negative of the equilibrium 30° C spectrum shown in Figure 1. Then, at each experimental time point, we multiplied the spectra by a time-dependent population function. We assumed that the changes in the population of e^-(aq) and I^-(aq) are governed by the recombination reaction ($I + e^- \rightarrow I^-$) and thus that the bleach recovery has the same time profile as the loss of the e^-(aq) transient absorption.

For the sake of simplicity, a kinetic model was used to describe this population dynamics and effectively parametrize the time-dependent population. The model was first proposed for the photodetachment problem by Staib and Borgis.[36] In other works, Bradforth and co-workers discussed more physical models for the ejection and recombination reaction.[37,38] Further, previous results for the magnitude and time scale of the electron solvation after detachment from iodide were used to approximate the electron thermalization, which must be included to fully describe the transient absorption signal due to the electron.[29,39]

The overall population dynamics that applies to the separated particles (I, e^-) and I^- recombination were fit from the electron population alone using the signal at the pump−probe transient absorption at 620 nm (2.0 eV), and the fit was confirmed for the other visible probe wavelengths. The competing kinetics model of Staib and Borgis employs the following parameters: contact pair formation rate, k_p; electron escape rate into the solution, k_d; and nonadiabatic geminate recombination rate to ground-state I^-, k_n.[36] The surviving population of electrons or iodine atoms as a function of time can be described by

$$\Omega_{SB}(t) = \frac{k_d}{k_d + k_n} + \frac{k_p}{k_d + k_n - k_p}\left[\frac{k_p - k_d}{k_p} e^{-k_p t} - \frac{k_n}{k_n + k_d} e^{-(k_d + k_n)t}\right] \quad (2)$$

The following parameters provide a good fit to the electron dynamics: $k_p^{-1} = 0.3$ ps, $k_n^{-1} = 42$ ps, and $k_d^{-1} = 32$ ps. This model provides a good description of the e^- population dynamics for the 100-ps time scale of this experiment. We note that these values are different from those found for I^-(aq) CTTS detachment at 255 nm.[37] The origins of this difference are discussed elsewhere.[38]

Figure 4b shows the time dependence of the remaining transients after the subtraction of the I^-(aq) and e^-(aq) contributions to the signal; the original full dataset is reproduced in Figure 4a. The I^-(aq) bleach was assumed to be instantaneous and to follow decay dynamics identical to that of the solvated electron. Similarly to the 10- and 100-ps time slices, there are residual transient absorptions near 5.9 eV (210 nm) and 5.2 eV (240 nm) with a broad shoulder on the red edge of the latter. This shoulder is once again similar to the $I(^2P_{3/2})$ atom aqueous charge-transfer absorption, although the residuals map shows some spectral evolution at early times out as far as 3.6 eV. This is more clearly revealed from inspection of the time transients in the region of the known I and predicted I* atom charge-transfer absorptions (between 4.8 and 3.6 eV). Absorption from 258 to 295 nm appears within the instrument response and decays with the same kinetics as the solvated electron and bleach. The decays at 310−344 nm are mostly over in ~1 ps and account for the evolution noted in Figure 4b. The nature of this spectral evolution prior to 10 ps is discussed in the next section.

Finally, to test whether immediate production of $I(^2P_{3/2})$ and its subsequent recombination with the electron can solely account for the entire 2D dataset, the $I(^2P_{3/2})$ absorption at 4.8 eV (260 nm) was subtracted from Figure 4b assuming a 1:1 stoichiometric ratio with both e^-(aq) and I^-(aq). The final residuals are shown in Figure 4c. In this step, $I(^2P_{3/2})$ was assumed to follow appearance and decay kinetics identical to those of e^-(aq). As judged by the residuals, the simple combination of the spectra of just three species following the same population dynamics successfully removed all intensity lower than 5.2 eV, at least after ~1 ps. The residual net absorption at all time delays near 5.9 eV resembles that observed in Figure 3. We note that the remaining striped structure at the far red and blue ends in the residuals plot overemphasizes the probe wavelength-to-wavelength uncertainty in the optical density scale after a strong signal has been subtracted. For example, residual absorption below 3.5 eV is within the 10% common ΔOD scale error bar due to the subtraction of the strong absorption of e^-(aq).[35]

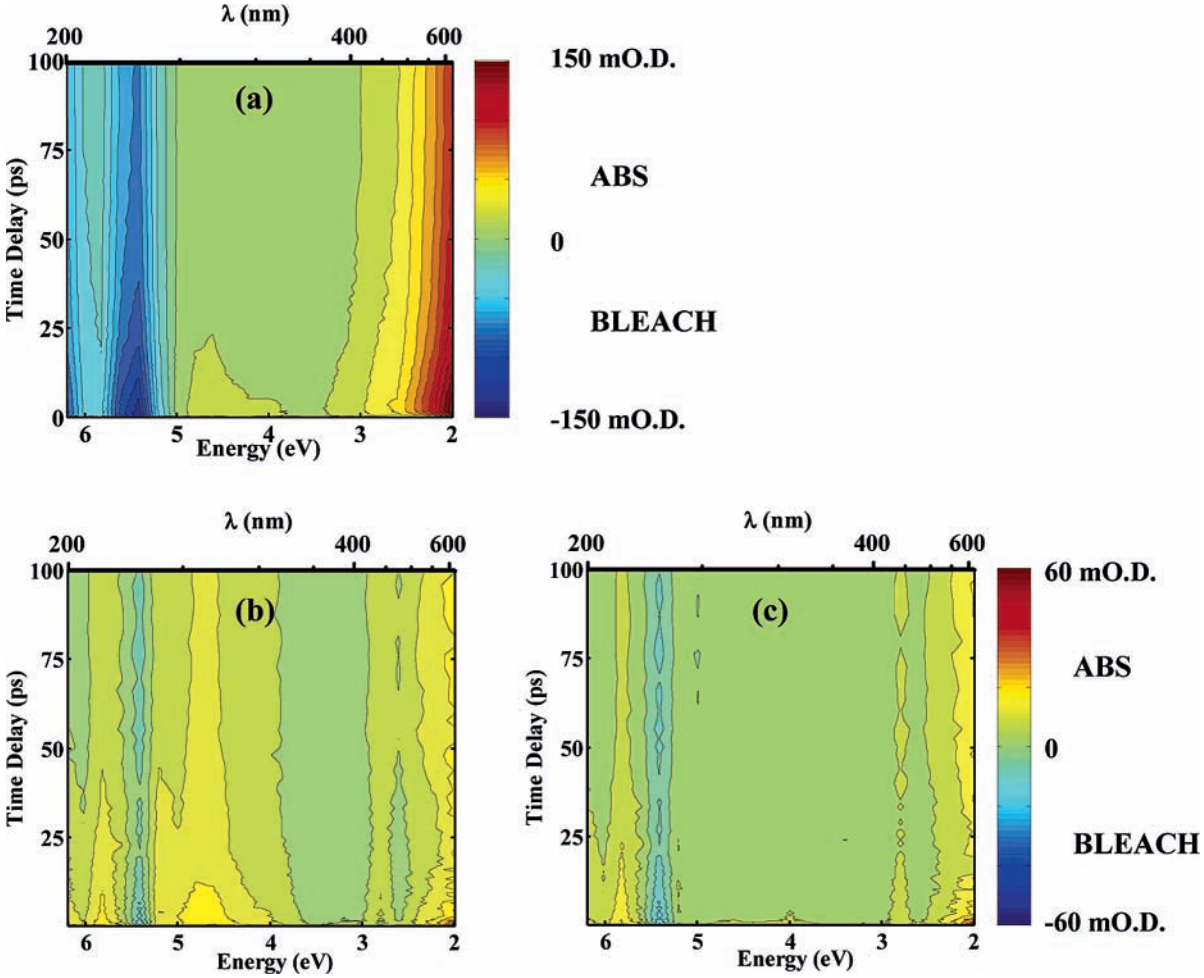

Figure 4. (a) Contour plot of the full experimental transient absorption dataset (identical to the projection in Figure 2). (b) Residual transient absorption after the dominant time-dependent contributions of e^-(aq) and I^-(aq) have been subtracted as described in the text. (c) Residual transient absorption after the I-atom charge-transfer contribution has also been subtracted from the experimental signal. The same false color scale is used for panels b and c.

V. Discussion

It is clear that the presented results show little evidence of the predicted I*(aq) absorption near 320 nm; however, the spectral signature of ground-state iodine atoms is clearly observed. In the following discussion, we first consider whether the spectroscopic prediction is in error, whether the I*($^2P_{1/2}$) state is quenched extremely rapidly in aqueous solution, or whether the detachment mechanism of the upper CTTS band is different from that of the lower CTTS band. Subsequently, we address the dynamics in the spectral region around the bleach.

Absence of a Signature for I*. First, Figure 3a clearly demonstrates that, by 10 ps, transient absorption from the e^-(aq) and ground-state I($^2P_{3/2}$) atom photoproducts and transient bleaching from the I^-(aq) atom are, within our experimental error, in a 1:1:1 stoichiometry. Thus, all initially excited I^-(aq) that has not recovered within 10 ps is present as a detached electron and I($^2P_{3/2}$), and there are no unexplained subpopulations. We can compare the relative magnitudes of each of these signals at earlier times. At 300 fs, we compute a ratio for e^-(aq) to bleached I^-(aq) of ~1.1. Therefore, even at very early times, every I^-(aq) that is excited leads to the production of a ground-state e^-(aq). This puts an upper limit on alternate possible pathways for the relaxation of CTTS excited I^-(aq), i.e., conversion to nondetaching triplet states or internal conversion back to the ground state. This suggests that the primary pathway for relaxation of the I^-(aq) excited state is indeed detachment of the electron, which is consistent with the estimates of a near-unity prompt electron quantum yield determined independently by Kloepfer et al. and Sauer et al.[18,37]

Recalling our motivation for this study, namely, to discern the absorption spectrum of aqueous I*($^2P_{1/2}$), we see little evidence for the predicted I* absorption near 320 nm. In addition, there are very few candidates for an I* band anywhere in the transient spectra once the I^- and e^- contributions have been removed. The only remaining transient absorptions occur at 260, 240, and 210 nm. The transient absorption at 260 nm very closely resembles the well-known ground-state I-atom charge-transfer absorption in water.[26,27] According to evidence provided later in this section, the two transient bands near 210 and 240 nm are most likely associated with differences in the re-formed I^-(aq) spectrum after the $I + e^-$ geminate recombination reaction. This leaves several possibilities with respect to I*: (i) I* and e^- undergo very fast recombination within the instrument response, leaving only e^- produced with ground-state I($^2P_{3/2}$); (ii) I* is deactivated on a time scale shorter than the experimental time resolution; or (iii) our initial assumption is incorrect, and excitation at 200 nm does not in fact produce separated iodine at the outset in its spin−orbit excited state. We rule out the possibility that I* is reacting with water, as there always remains good stoichiometric equivalence between electrons and iodine species in the observed transients. Of course, we cannot exclude the possibility that the aqueous I*

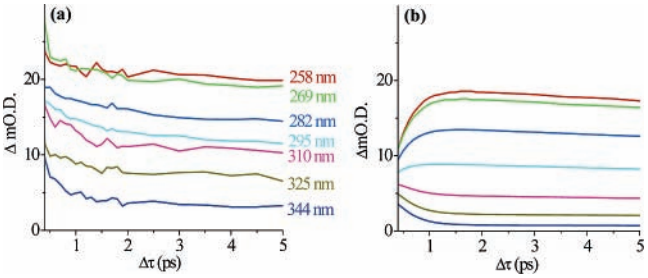

Figure 5. (a) Residual pump−probe transient absorption after the I^- and e^- time-dependent contributions have been subtracted. Probe wavelengths from 258 to 344 nm in the region of the known $I(^2P_{3/2})$ charge-transfer absorption and the predicted $I^*(^2P_{1/2})$ absorption. (b) Simulation from a simple two-level kinetic system for I* → I relaxation assuming that I*(aq) has a charge-transfer absorption at 320 nm and an I* → I conversion time scale of 300 fs. At all times, the experimental results show the strongest residual absorption near the ground-state I absorption maximum at 260 nm. There is an additional fast decay component in the redder probe wavelengths, but there does not appear to be a corresponding rise near 260 nm as expected for I* → I relaxation in the two-state model.

charge-transfer absorption band perfectly overlaps the charge-transfer absorption of ground-state I, but we consider that possibility highly unlikely.

In possibility i, we posit that I* is being quenched by electron transfer[40,41] (i.e., $I^* + e^-$) to re-form I^- faster than the instrument response and that the observed signals correspond only to those geminate pairs formed when iodine is produced in its ground state. We find this possibility unlikely, as the magnitude of the recorded bleach and electron signals suggests that ∼25% of the total iodide ions in the solution remain bleached after 300 fs. In addition, the prompt electron quantum yield, namely, the number of electrons detected immediately after an ultrafast (∼300-fs) excitation pulse, has recently been measured at 200 nm independently and found to be 90%.[18] From these two facts, we can conclude that, even if a fast $I^* + e^-$ reaction were active, this can account for only a very small fraction of the population. Finally, if anything, we would expect $I^*(^2P_{1/2})$ to react more slowly than the tens-of-picoseconds time scale for $I(^2P_{3/2})$. This is because the recombination reaction is likely in the Marcus inverted regime (see below) and electron transfer to I* is even more downhill than that to the ground-state I atom.[37,42,43]

To consider the argument for a short lifetime for I* in water (possibility ii), we examined the early pump−probe transient signals in the region of the $I(^2P_{3/2})$ charge-transfer absorption at 260 nm and the predicted $I^*(^2P_{1/2})$ charge-transfer absorption near 320 nm shown in Figure 5a. The maxima of the observed $I(^2P_{3/2})$ and predicted $I^*(^2P_{1/2})$ charge-transfer absorption bands in water are at 260 and 320 nm, respectively.[2,26,27] An additional fast decay is observed in the 295−344-nm experimental transients in the region of the predicted I* band. No corresponding rise is evident in the transients near 260 nm to suggest I* → I conversion. To explore whether the observed transients are consistent with the predicted band position for I* and near-instrument-limited conversion, we carried out a simple simulation. Figure 5b shows a simulation of the transient signals in this region for I* → I conversion on a 300-fs time scale, assuming that the putative I* absorption at 320 nm has the same strength and width as the 260-nm ground-state I-atom charge-transfer band. These simulations were created by using the kinetic model from eq 2 to describe the total population of I + I*. The literature $I(^2P_{3/2})$ absorption spectrum was used, and the I* spectrum was created by simply red shifting the same spectrum by the spin−orbit splitting of gas-phase iodine. The fractional populations of I and I* were modeled with an exponential rise and decay, respectively ($\tau \sim 300$ fs). Comparing the residual data in Figure 5a and b, we see that the simulation well reproduces the 310-, 325-, and 344-nm transients in the region of the predicted I* absorption. However, in the $I(^2P_{3/2})$ region, the simulation shows a strong rise corresponding to the appearance of ground-state I that is clearly absent in the experimental results. This suggests that, if I* really does absorb in the 320-nm region, the lifetime of I*(aq) is shorter than 300 fs following 200-nm detachment of I^-(aq). If the other scenarios described in this section are correct, Figure 5a would instead be taken as evidence for spectral evolution or narrowing within the $I(^2P_{3/2})$ band, for example, as a result of solvent reorientation. Elles et al. observed a small narrowing and shifting of the absorption by the Cl-atom charge-transfer complex with CH_2-Cl_2 after the initial complex formation following CH_3OCl photodissociation in that solvent.[44]

Before moving on to consider a final explanation, it is worth critically considering whether electronic relaxation processes on the order of 300 fs are feasible according to the extensive literature for the I* species. To date, no experimental lifetime has been reported for I* in a room-temperature liquid. In rare-gas matrixes, the I* lifetime is ∼5 ms,[45] whereas a lower bound on the free I* lifetime in CCl_4 is ∼1 μs.[46,47] The relaxation rate can be strongly enhanced through quasiresonant electronic-to-vibrational energy transfer involving quadrupole−dipole coupling.[48−51] The highest rates occur when the energy gap between the I* → I transition and the acceptor mode is small, such as when water is the acceptor (with two quanta accepted into the OH stretching mode). Use of a binary collision model and that gas-phase rate for I* deactivation with H_2O leads to an estimate of ∼160 collisions required to deactivate I*.[50,51] This still corresponds to ∼16 ps in room-temperature water, considerably slower than necessary to account for our experimental results. However, electronic-to-vibrational energy transfer is highly dependent on the spectral overlap between the acceptor vibrational spectrum and the I*−I energy gap. Following the photoexcitation of I^-(aq), there are two species near the iodine atom, water and the electron. If the electron were to enhance the electronic relaxation rate of I*, it would most likely do so by its indirect effect on the vibrational spectrum of the nearby water molecules. The presence of a nearby excess electron is known to red shift the OH stretch and the bending frequencies in water[52−55] and likely will increase the anharmonicity, thereby increasing the overtone strength. Additionally, from the data of Johnson and co-workers for hydrated electron clusters, the fundamental band intensities appear to be enhanced when the OH bond is pointed toward an excess electron, although the magnitude of the enhancement has yet to be quantified.[52,56] A bulk solvated electron enhances the Raman stretch and bend fundamentals by 3−5 orders of magnitude; however, because the Raman cross section is resonantly enhanced by the solvated-electron transition, we cannot easily quantify the transition strength from these data.[53−55] As the coupling element for electronic-to-vibrational energy transfer is dependent on the accepting water vibrational transition dipole strength, this would suggest that the efficiency of I* deactivation might be enhanced if the solvated electron is close to the accepting water. This analysis suggests that solvents with a hydrogen stretching mode can lead to unusually fast deactivation and that the presence of a nearby electron can further enhance the condensed phase rate, although it is not clear that a rate as high as 10^{13} s^{-1} would be expected.

We now consider possibility iii, that one of the premises for our experiment, that a distinct I* radical is generated from

excitation to the second CTTS band, is flawed despite the prior assignments of the vertical upper state as $5p^5(^2P_{1/2})6s$. It is certainly possible that additional processes outcompete the adiabatic separation of the CTTS electron to an $I^*:e_{solv}$ caged pair, the paradigm that has been developed for the lowest CTTS state.[37,57,58] For example, the CTTS state can itself undergo internal conversion, effectively electronically relaxing the iodine core before the CTTS electron has separated.[57] Alternatively, the vertically excited state might be indirectly coupled into the electron detachment continuum corresponding to $I(^2P_{3/2})$ and a water conduction band electron,[38] which necessitates an iodine J state change—this is a spin−orbit-induced autodetachment process analogous to that observed for gas-phase anions.[59] Autoionization processes have recently been invoked to explain photoionization processes in water.[60] Bradforth and co-workers have argued, on the basis of recent liquid jet photoelectron spectroscopy,[61] that the water conduction band might be energetically accessible at 200 nm when associated with an $I(^2P_{3/2})$ hole but not with an $I(^2P_{1/2})$ hole. Both the internal conversion and autodetachment mechanisms circumvent the formation of $I(^2P_{1/2})$ and account for the early appearance of the $I(^2P_{3/2})$ absorption band. However, if internal conversion is taking place prior to electron ejection, the ejection length characterized by the time-dependent recombination of the electron and now $I(^2P_{3/2})$ geminate pair would be expected to resemble that observed when the lowest CTTS is excited directly. As briefly noted in section IV and described in great detail in a separate article,[38] geminate recombination recorded at 200 nm [as evidenced by the identical time evolutions of the bleach recovery, $I(^2P_{3/2})$, and solvated-electron populations here] is *very different* from that observed when the lowest CTTS state is excited at 255 or 225 nm. A similar argument would apply to possibility i, for geminate recombination with a separated iodine atom that has been electronically relaxed by the solvent.

As autodetachment directly yields $I(^2P_{3/2})$ and simultaneously provides a rationale for both the different geminate recombination kinetics observed[38] and the absence of an absorption band attributable to I*, this is our preferred explanation for the current experimental results. In the other two plausible scenarios, I*, either as the core within the initial CTTS state or after formation of a contact pair with the solvated electron, must undergo <300-fs electronic relaxation, and additionally, the different geminate recombination kinetics must be explained by an increased local temperature resulting from the ~0.9-eV energy deposited in the electronic relaxation step.[62,63]

Cooling of the Re-formed I^-(aq). Figure 2 shows that, above 100-ps, a substantial fraction of the electrons and iodine radicals recombine to re-form iodide and thus the I^-(aq) ground-state bleach slowly recovers on the same time scale. The recombination reaction is an electron-transfer (ET) process that can be described by Marcus theory. In previous work, the USC group showed that the return ET reactions for halide CTTS systems are in the inverted regime, that is, the reaction rate decreases as the driving force, $\Delta G°$, increases[42] or the solvent reorganization decreases as the solvent polarity decreases.[43] According to quantum-corrected Marcus theory, electron transfer in the inverted regime is accelerated for reactions yielding a vibrationally excited product such that there is a closer match in the net free energy released and the solvent reorganization energy.[64] High-frequency vibrational modes in the acceptor are particularly effective in enhancing the inverted-regime reaction rate. For an atomic acceptor, the promoting vibrational modes thus must be the tightly coupled stretching vibrations of the first-shell water molecules. This idea is supported by the observation

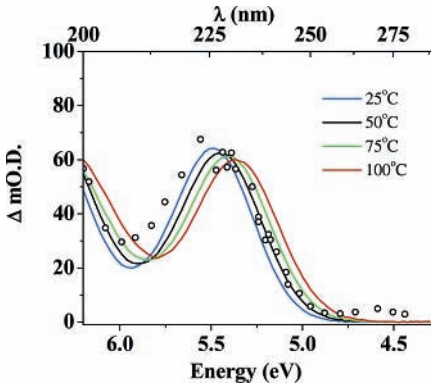

Figure 6. Transient absorption spectrum of recombined iodide at 100 ps compared to the steady-state absorption spectrum of aqueous iodide at various temperatures (from ref 67). The transient spectrum was derived from the experimental transient by removal of solvated-electron and the I-atom charge-transfer contributions (in proportion to their concentration at 100 ps) and addition of the steady-state 30 °C iodide spectrum scaled to account for the *entire* initially bleached population; the spectrum of the bleach recovery thus shows as a positive absorption band. Although the recombined iodide band is centered near the peak of the equilibrium 30 °C spectrum, there appears to be considerable broadening on both sides of the band.

that the recombination rate between I and e^-(aq) is almost a factor of 2 lower in D_2O than in H_2O.[65]

The intramolecular vibrational energy deposited by the electron-transfer reaction will likely be rapidly relaxed as a result of the properties of the hydrogen-bonding network of water. For example, relaxation of $\upsilon_{stretch} = 1$ for water molecules surrounding I^-(aq) occurs on a ~2-ps time scale.[66] Here, larger numbers of quanta of vibration are expected to be deposited in the first shell of water, given that $\Delta G° \approx 4.2$ eV,[43] although the vibrational relaxation is still likely to be considerably more rapid than the electron-transfer reaction. The excess vibrational energy will be dissipated through the water network, resulting in a local temperature increase near the newly formed I^-(aq) anion. However, the long-time temperature jump expected throughout a thermally equilibrated solution inside the pump laser spot should amount to only <1 K under our experimental conditions (assuming ~1 μJ absorbed and an excitation volume of water of $\sim 10^{-2}$ μL). As the absorption spectrum of thermalized I^-(aq) is strongly dependent on temperature,[20,23,24] we can thus potentially probe to see how rapidly the local temperature jump is dissipated in the form of the bleach recovery.

We compare the absorption spectrum of re-formed iodide ("hot iodide") at 100 ps to the equilibrium absorption spectra in Figure 6. The transient spectrum for the recombined anion was derived considering that the entire population of bleached molecules can be characterized by the ambient temperature before the pump pulse (30°C) whereas the species filling in the bleach have a spectrum associated with hot recombined anions. The steady-state spectra are from recent unpublished data from Marin and Bartels, who obtained spectra of I^-(aq) at up to 100°C and 250 bar, as well as spectra under supercritical conditions.[67] Their spectra were carefully controlled for the onset of water absorption near 200 nm. Under 100 °C, the density of water at this pressure is very similar to that of water at 1 atm. Thus, these new spectra, which extend to higher temperatures than the most detailed spectra in the literature,[23,24] provide us with the most useful comparison.[68]

Figure 6 shows that the absorption spectrum for re-formed iodide is wider than any of the equilibrium spectra, accounting for the excess absorption at 210 and 240 nm described in section

IV. However, the peak center is close to that of the spectrum for ambient-temperature conditions (30 °C), suggesting that energy dissipation is extremely rapid. The additional width on both the blue and red sides of the spectrum is surprising; a red-shifted spectrum would have been understandable in terms of incomplete local cooling. This limits the conclusions that we can make at this stage about how energy flows from the first shell into the bulk. It is perhaps noteworthy to point out that there is no noticeable spectral shifting or narrowing in the time evolution of the recovering iodide bleach (as can be inferred from Figure 4c). This suggests that the thermal diffusion rate is considerably higher than the rate of the electron-transfer reaction (40 ps) that deposits the vibrational energy.

VI. Conclusions

We see no evidence of a charge-transfer absorption between water and $I^*(^2P_{1/2})$ following preparation of I* by 200-nm photodetachment of I^-(aq). The most likely explanation for the missing I* absorption amounts to unexpected nonadiabatic relaxation pathways for either the iodide or iodine excited states. Deactivation of $I^*(^2P_{1/2})$ either during or after destruction of the CTTS state could be taking place on a sub-300-fs time scale, or the initial CTTS state might be decaying by autodetachment into $I(^2P_{3/2})$ and a conduction-band electron. The autodetachment mechanism explains the fact that the ejection length, recovered from analysis of the ensuing geminate recombination dynamics, is greater than that observed upon excitation into the lowest CTTS band. If the mechanism is instead electronic relaxation of I*, it most likely takes place by electronic-to-vibrational energy transfer, with the first-shell water stretching vibration, enhanced by the diffuse electron, as the energy-accepting mode. Whether this time scale represents the natural lifetime of I* in water and is thus pertinent to the relaxation of I* after photodissociation of aqueous ICN depends strongly on the role of the nearby solvated electron in enhancing the energy transfer. Searching for signatures of I* when the electron is ejected to far greater radii by photodetaching I^- above 8 eV[38] might help to both eliminate the possibility of electron-enhanced relaxation of I* and connect directly to the I* detachment continuum.[61] Our joint interpretation of the impact of these and other recent results on the photodissociation of ICN will be consolidated elsewhere.[69]

The observation that I* is not produced (either by subpicosecond electronic relaxation or through autodetachment) is significant in understanding the photodetachment mechanism of iodide. It implies that that all geminate recombination (taking place on the tens-of-picoseconds time scale) of the solvated electron is with ground-state iodine radicals and this should occur at the same on-contact rate as observed for longer-wavelength photodetachment.[70] Further, the observation that the spectrum of the re-formed iodide anion can be characterized by a near-ambient temperature illustrates that vibrational relaxation and thermal cooling are fast compared to the reverse electron-transfer reaction; the hydrogen-bonding network appears to be able to rapidly accommodate ~5 eV of vibrational energy. This study highlights the unique role of the high-frequency stretching modes of water, which can simultaneously act to rapidly relax electronic excitation in the I* radical by resonant electronic-to-vibrational energy transfer and then accelerate the return reaction of the solvated electron to the iodine parent while, by excellent coupling to the surrounding hydrogen-bonding network, transferring excess energy away from the primary solvent shell within 10 ps.

Acknowledgment. We thank Tim Marin and David Bartels for sharing their temperature-dependent spectra of I^-(aq) prior to publication and Mark Johnson for stimulating discussions. The work at USC was supported by the U.S. National Science Foundation (CHE-0311814). S.E.B. is a Fellow of the David and Lucile Packard Foundation. J.T. and S.K. thank the Lundbeck Foundation and the Danish National Research Council for financial support.

References and Notes

(1) Moskun, A. C.; Bradforth, S. E. *J. Chem. Phys.* **2003**, *119*, 4500.
(2) Larsen, J.; Madsen, D.; Poulsen, J.-A.; Poulsen, T. D.; Keiding, S. R.; Thøgersen, J. *J. Chem. Phys.* **2002**, *116*, 7997.
(3) Thogersen, J.; Jensen, S. J. K.; Christianson, O.; Keiding, S. R. *J. Phys. Chem. A* **2004**, *108*, 7483.
(4) Thomsen, C. L.; Madsen, D.; Thogersen, J.; Byberg, J. R.; Keiding, S. R. *J. Chem. Phys.* **1999**, *111*, 703.
(5) Buxton, G. V.; Subhani, M. S. *J. Chem. Soc., Faraday Trans. 1* **1972**, *68*, 947.
(6) Hug, G. L. *Optical Spectra of Nonmetallic Inorganic Transient Species in Aqueous Solution*; U.S. Department of Commerce, National Bureau of Standards: Washington, DC, 1981.
(7) Grajower, R.; Jortner, J. *J. Am. Chem. Soc.* **1962**, *85*, 512.
(8) Chestakov, D. A.; Wu, S. M.; Wu, G. R.; Parker, D. H.; Eppink, A.; Kitsopoulos, T. N. *J. Phys. Chem.* **2004**, *108*, 8100.
(9) Samartzis, P. C.; Bakker, B. L. G.; Rakitzis, T. P.; Parker, D. H.; Kitsopoulos, T. N. *J. Chem. Phys.* **1999**, *110*, 5201.
(10) Person, M. D.; Kash, P. W.; Butler, L. J. *J. Chem. Phys.* **1991**, *94*, 2557.
(11) Zhang, J.; Dulligan, M.; Segall, J.; Wen, Y.; Wittig, C. *J. Phys. Chem.* **1995**, *99*, 13680.
(12) Chastaing, D.; Underwood, J.; Wittig, C. *J. Chem. Phys.* **2003**, *119*, 928.
(13) Zhang, J.; Dulligan, M.; Wittig, C. *J. Chem. Phys.* **1997**, *107*, 1403.
(14) Moskun, A. C.; Jailaubekov, A. E.; Bradforth, S. E.; Tao, G.; Stratt, R. M. *Science* **2006**, *311*, 1907.
(15) Pieniazek, P. A.; Bradforth, S. E.; Krylov, A. I. *J. Phys. Chem. A* **2006**, *110*, 4854.
(16) Jortner, J.; Ottolenghi, M.; Stein, G. *J. Phys. Chem.* **1963**, *67*, 1271.
(17) Kloepfer, J. A. Ultrafast Dynamics of Iodide Photodetachment. Ph.D. Dissertation, University of Southern California, Los Angeles, CA, 2002.
(18) Sauer, M. C.; Crowell, R. A.; Shkrob, I. A. *J. Phys. Chem. A* **2004**, *108*, 5490.
(19) Jortner, J.; Raz, B.; Stein, G. *Trans. Faraday Soc.* **1960**, *56*, 1273.
(20) Blandamer, M.; Fox, M. *Chem. Rev.* **1970**, *70*, 59.
(21) Orgel, L. E. *Q. Rev. Chem. Soc.* **1954**, *8*, 422.
(22) Fox, M. F. *Q. Rev. Chem. Soc.* **1970**, *24*, 565.
(23) Fox, M. F.; Hayon, E. *J. Chem. Soc., Faraday Trans. 1* **1977**, *73*, 1003.
(24) Fox, M. F.; Barker, B. E.; Hayon, E. *J. Chem. Soc., Faraday Trans. 1* **1978**, *74*, 1776.
(25) Jou, F.-Y.; Freeman, G. R. *J. Phys. Chem.* **1979**, *83*, 2383.
(26) Fornier de Violet, P. *Rev. Chem. Int.* **1981**, *4*, 121.
(27) Fornier de Violet, P.; Bonneau, R.; Joussot-Dubien, J. *Chem. Phys. Lett.* **1973**, *19*, 521.
(28) Madsen, D.; Thomsen, C. L.; Thogersen, J.; Keiding, S. R. *J. Chem. Phys.* **2000**, *113*, 1126.
(29) Vilchiz, V. H.; Kloepfer, J. A.; Germaine, A. C.; Lenchenkov, V. A.; Bradforth, S. E. *J. Phys. Chem. A* **2001**, *105*, 1711.
(30) Moore, C. E. *Atomic Energy Levels*; National Bureau of Standards: Washington, DC, 1971.
(31) Mulliken, R. R. *J. Am. Chem. Soc.* **1952**, *74*, 811.
(32) Weissbluth, M. *Atoms and Molecules*; Academic Press: New York, 1978.
(33) Madsen, D.; Larsen, J.; Jensen, S. J. K.; Keiding, S. R.; Thogersen, J. *J. Am. Chem. Soc.* **2003**, *125*, 15571.
(34) Wang, Z. H.; Shoshana, O.; Hou, B. X.; Ruhman, S. *J. Phys. Chem. A* **2003**, *107*, 3009.
(35) The small remaining absorption seen in the black circle trace at wavelengths longer than 500 nm likely corresponds to additional solvated electrons generated by ionization of the water, as described in section III.
(36) Staib, A.; Borgis, D. *J. Chem. Phys.* **1996**, *104*, 9027.
(37) Kloepfer, J. A.; Vilchiz, V. H.; Lenchenkov, V. A.; Germaine, A. C.; Bradforth, S. E. *J. Chem. Phys.* **2000**, *113*, 6288.
(38) Chen, X.; Kloepfer, J. A.; Bradforth, S. E.; Lian, R.; Crowell, R. A.; Shkrob, I. A., manuscript in preparation.
(39) We note that, although the characterized electron thermalization following detachment in the first CTTS band at 255 nm can be satisfactorily used for the current dataset (400−620 nm), the e^-(aq) thermalization

following 200-nm I^-(aq) photodetachment appears to be slightly better described by shortening the relaxation time from 850 fs by ~20% or decreasing the initial spectral shift from 0.36 eV by ~40%.

(40) Sanov, A.; Faeder, J.; Parson, R.; Lineberger, W. C. *Chem. Phys. Lett.* **1999**, *313*, 812.

(41) Sanov, A.; Sanford, T.; Nandi, S.; Lineberger, W. C. *J. Chem. Phys.* **1999**, *111*, 664.

(42) Vilchiz, V. H. Electron Photodetachment from Singly Charged Anions. Ph.D. Dissertation, University of Southern California, Los Angeles, CA, 2002.

(43) Vilchiz, V. H.; Chen, X. Y.; Kloepfer, J. A.; Bradforth, S. E. *Radiat. Phys. Chem.* **2005**, *72*, 159.

(44) Elles, C. G.; Cox, J.; Barnes, G. L.; Crim, F. F. *J. Phys. Chem. A* **2004**, *108*, 10973.

(45) Chichinin, A. I. *J. Phys. Chem. Ref. Data* **2006**, *35*, 869.

(46) Benderskii, A. V.; Zadoyan, R.; Apkarian, V. A. *J. Chem. Phys.* **1997**, *107*, 84378445.

(47) Zadoyan, R.; Sterling, M.; Ovchinnikov, M.; Apkarian, V. A. *J. Chem. Phys.* **1997**, *107*, 8446.

(48) Chiappero, M. S.; Badini, R. G.; Arguello, G. A. *Int. J. Chem. Kinet.* **1996**, *29*, 155.

(49) Chiappero, M. S.; Arguello, G. A. *Int. J. Chem. Kinet.* **1998**, *30*, 799.

(50) Donovan, R. J.; Fotakis, C.; Golde, M. F. *Faraday Discuss. Chem. Soc.* **1976**, 2055.

(51) Donovan, R. J.; Husain, D. *Trans. Faraday Soc.* **1966**, *62*, 2023.

(52) Hammer, N. I.; Shin, J. W.; Headrick, J. M.; Diken, E. G.; Roscioli, J. R.; Weddle, G. H.; Johnson, M. A. *Science* **2003**, *306*, 675.

(53) Tauber, M. J.; Mathies, R. A. *J. Phys. Chem. A* **2001**, *105*, 10952.

(54) Tauber, M. J.; Mathies, R. A. *Chem. Phys. Lett.* **2002**, *354*, 518.

(55) Tauber, M. J.; Mathies, R. A. *J. Am. Chem. Soc.* **2003**, *125*, 1394.

(56) Johnson, M. A. Yale University, New Haven, CT. Private communication, 2005.

(57) Sheu, W.-S.; Rossky, P. J. *J. Phys. Chem.* **1996**, *100*, 1295.

(58) Lehr, L.; Zanni, M. T.; Frischkorn, C.; Weinkauf, R.; Neumark, D. M. *Science* **1999**, *284*, 635.

(59) Andersen, T.; Lykke, K. R.; Neumark, D. M.; Lineberger, W. C. *J. Chem. Phys.* **1987**, *86*, 1858.

(60) Elles, C. G.; Jailaubekov, A. E.; Crowell, R. A.; Bradforth, S. E. *J. Chem. Phys.* **2006**, *125*, 044515.

(61) Winter, B.; Weber, R.; Hertel, I. V.; Faubel, M.; Jungwirth, P.; Brown, E. C.; Bradforth, S. E. *J. Am. Chem. Soc.* **2005**, *127*, 7203.

(62) Dessent, C. E. H.; Bailey, C. G.; Johnson, M. A. *J. Chem. Phys.* **1995**, *103*, 2006.

(63) Iglev, H.; Trifonov, A.; Thaller, A.; Buchvarov, I.; Fiebig, T.; Laubereau, A. *Chem. Phys. Lett.* **2005**, *403*, 198.

(64) Barbara, P. F.; Meyer, T. J.; Ratner, M. A. *J. Phys. Chem.* **1996**, *100*, 13148.

(65) Kloepfer, J. A.; Bradforth, S. E., manuscript in preparation.

(66) Kropman, M. F.; Bakker, H. J. *J. Am. Chem. Soc.* **2004**, *126*, 9135.

(67) Martin, T.; Argonne National Lab, Argonne, IL; Bartels, D. M. Notre Dame Radiation Lab, South Bend, IN. Private communication, 2005.

(68) Temperature-dependent absorption maxima of the first I^-(aq) CTTS band for temperatures up to 373 K from Marin and Bartels match within 1 nm of the absorption maxima predicted by extrapolations of Fox and Hayon's data obtained at atmospheric pressure from 298 to 343 K.

(69) Thogersen, J.; Knak, S.; Keiding, S. R.; Moskun, A. C.; Pieniazek, P.; Krylov, A. I.; Bradforth, S. E., manuscript in preparation.

(70) Kloepfer, J. A.; Vilchiz, V. H.; Lenchenkov, V. A.; Chen, X.; Bradforth, S. E. *J. Chem. Phys.* **2002**, *117*, 766.